

# Effects of the tool rotational speed and shoulder penetration depth on mechanical properties and failure modes of friction stir spot welds of aluminum 2024-T3 sheets<sup>†</sup>

Moslem Paidar<sup>1,\*</sup>, Alireza Khodabandeh<sup>2</sup>, Hamidreza Najafi<sup>2</sup> and Alireza Sabour Rouh-aghdam<sup>3</sup>

<sup>1</sup>Department of Materials Engineering, South Tehran Branch, Islamic Azad University, Tehran, Iran

<sup>2</sup>Department of Materials Engineering, Science and Research Branch, Islamic Azad University, Tehran, Iran

<sup>3</sup>Department of Materials Engineering, Tarbiat Modares University, Tehran, Iran

(Manuscript Received January 24, 2014; Revised August 5, 2014; Accepted August 31, 2014)

## Abstract

In this work, friction stir spot welding with 1.6 mm thickness of the 2024-T3 aluminum alloy is carried out. The effects of the tool rotational speed and shoulder penetration depth on surface appearance, macrostructure, temperature profile, maximum failure load and failure modes are investigated. Results show that, the effect of the tool rotational speed on maximum tensile shear load is similar to the effect of the shoulder penetration depth, increasing tool rotational speed and shoulder penetration depth resulted in the increase of the tensile shear load. Maximum load of about 8282 N is obtained by using 1000 rpm rotational speed and 0.7 mm shoulder penetration depth. Observation of the failed specimens indicates two types of failure modes under tensile shear loading, the shear fracture that occurs in low shoulder penetration depths and tensile shear fracture that occurs in high shoulder penetration depths.

*Keywords:* Failure modes; Friction stir spot welding; Shoulder penetration depth; Tool rotational speed

## 1. Introduction

Friction stir spot welding (FSSW) new process that utilized for applications in aerospace, automotive and other industrial applications [1]. In 2001, friction stir spot welding was developed in the automotive industry to substitute resistance spot welding (RSW) for aluminum sheet [2]. As shown schematically in Fig. 1, FSSW technology including three steps: plunging, stirring and retracing [3]. A rotating tool with a probe pin is first inserted into the upper sheet. When the rotating tool contacts the upper sheet, a tool downward force is applied [4]. Upon reaching the desired penetration depth, the rotating tool is held in that position for a pre-determined finite time (sometimes referred to as dwell time). Subsequent to that, the rotating tool is then retracted from the welded joint leaving behind a friction stir spot weld. FSSW can be considered as a transient process due to its short cycle time (usually a few seconds). During FSSW, tool penetration and the dwell period essentially determine the heat generation, material plasticization around the pin, weld geometry and therefore mechanical properties of the welded joint [5]. Several studies investigated the effect of different parameters on failure load of joints. For example, Lathabi et al. [6] observed that increasing tool rotational speed in FSSW, initially increased welds strength but

then decreased, while Tozaki et al. [7] found that the welds tensile shear strength decreased with increasing tool rotational speed. Pan et al. [8] and Fujimoto et al. [9, 10] found that the failure load and failure modes depending to the tool insertion depths. Also, Pathak et al. [11] found that weld tensile shear load increased with increasing the rotational speed and penetration depth. Yoon et al. [12] reported that the increase at tool penetration depth leading to increase the tensile shear load. Studies have also been reported the effects welding parameters on failure mode. Lathabai [6] and Tozaki [7] found that in the FSSW under tensile shear loading presents two failure modes. Mitlin et al. [13] have reported the effect of tool pin penetration depth on the fracture type: With increasing penetration depth, the fracture location shifts away from the pin toward the base metal. It is well known that the penetration depth and tool rotational speed, playing a major role in determining the weld quality and failure modes. In this paper, the effects of the shoulder penetration depth (0.3, 0.5 and 0.7 mm) and tool rotational speed (630, 1000 and 1600 rpm) on surface appearance, macrostructure, temperature profile, maximum failure load and failure modes were investigated.

## 2. Material and methods

The 2024-T3 aluminum alloy sheets with 1.6 mm thickness were used in this investigation. The chemical composition and mechanical properties as-received sheets given in Tables 1

\*Corresponding author. Tel.: +98 2144507106, Fax.: +98 2144507106

E-mail address: M.Paidar@srbiau.ac.ir

<sup>†</sup> Recommended by Associate Editor Chongdu Cho

Table 1. Chemical composition of AA2024-T3 (wt%).

	Al	Cu	Mg	Mn	Ti	Zn	Fe
Bulk	4.9	1.28	0.629	0.0154	0.142	0.239	

Table 2. Mechanical properties of AA2024-T3.

Elongation (%)	Yield strength (MPa)	Tensile strength (MPa)
18 ~	322 ~	450

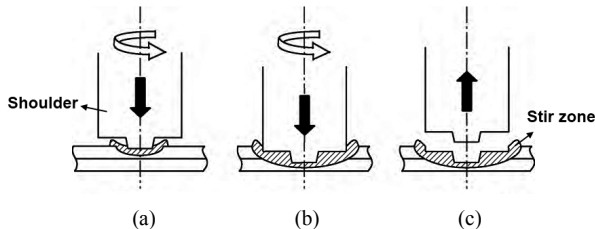


Fig. 1. Schematic of welding by FSSW: (a) plunging; (b) stirring; (c) retracting.

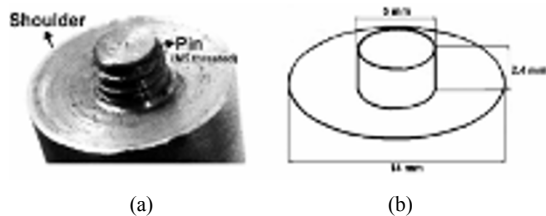


Fig. 2. (a) A photo of a tool; (b) a schematic illustration of FSSW tool geometries.

and 2, respectively.

The tool was made of H13 steel with hardness of  $50 \pm 2$  HRC and the concavity angle of  $8^\circ$ . Diameter and length of pin were 5 mm and 2.4 mm, respectively (see Fig. 2). Also diameter of shoulder was considered 14 mm. The tool rotational speeds and shoulder penetration depths change respectively in 630, 1000 and 1600 rpm with 0.3, 0.5 and 0.7 mm.

A constant penetration rate and dwell time were applied: 2 mm/min and 5 s, respectively.

Welded tensile shear specimens were tested on an Instron machine at a constant cross head speed of 3 mm/min. Both specimens were made by using two sheets of  $100 \times 25$  mm with an overlap area of  $25 \times 25$  mm. Tensile shear tests was carried out according to AWS C1.1: 2007 standard. The specimens were welded in a milling machine. In order to develop the FSSW tests, a properly designed clamping fixture was utilized to fix the specimens. During welding, the temperature under the pin was recorded by thermocouple (K-type) in the anvil (see Fig. 4). During metallography, the weld samples were polished by using  $0.3 \mu\text{m}$  alumina suspension and then etched with Keller's reagent (1ml HF, 1.5 ml HCl, 2.5 ml  $\text{HNO}_3$ , 95 ml  $\text{H}_2\text{O}$ ) for 40 s. Microstructure was examined by using OLYMPUSE optical microscope and VEGATESCAN scanning electron microscope. Also, EDX analysis was performed on a selected area.

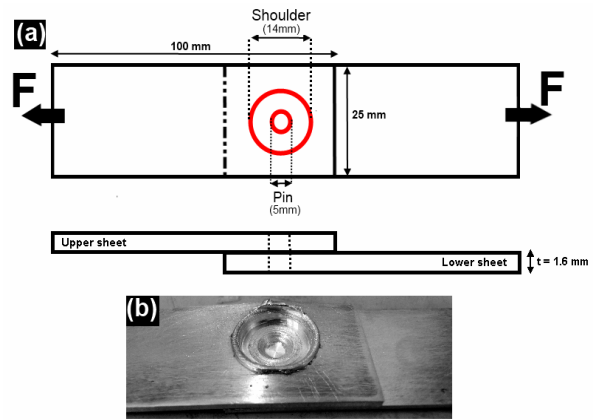


Fig. 3. Tensile shear specimen: (a) schematic illustration with dimensions; (b) photo after FSSW. The arrows indicate the loading direction.

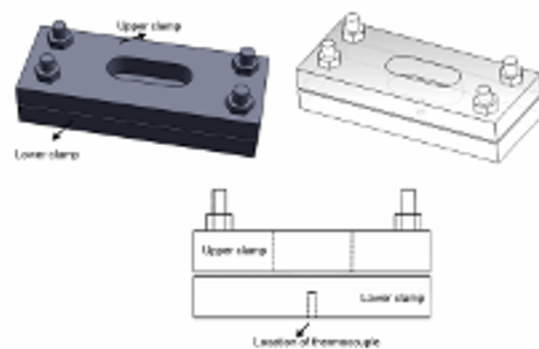


Fig. 4. A schematic illustration of the specimen fixture and location of thermocouple.

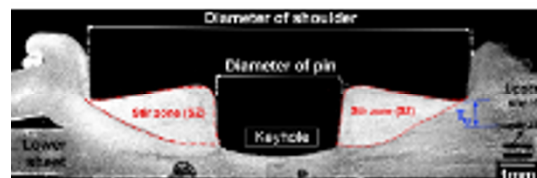


Fig. 5. Cross-sectional macrostructure of a typical friction stir spot weld illustrating the different weld geometrical features.

### 3. Results and discussion

Fig. 5 depicts the geometrical features of friction stir spot welding. "Keyhole" which was produced with the pull out tool in joint. "Stir zone" which contains equiaxed fine grains caused by the full dynamic recrystallization took place in the vicinity of the rotating pin [14]. The stir zone area determines the strength of welds [12, 15]. In addition, "the thickness of the upper sheet under the shoulder indentation ( $T_u$ )" that is defined as the distance between the shoulder indentation and interface of upper and lower sheets is indicated in Fig. 5.

It has been reported that  $T_u$  is a key factor that determines the strength of joints [16] and failure modes [7].

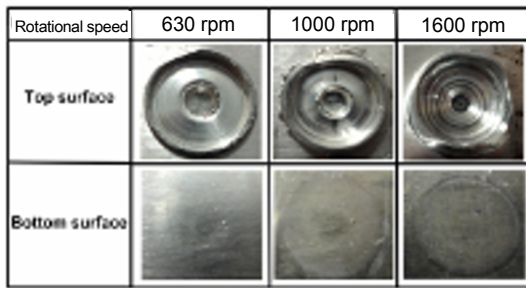


Fig. 6. The effect of tool rotational speed on surface appearance welded specimens at 0.3 mm penetration depth.

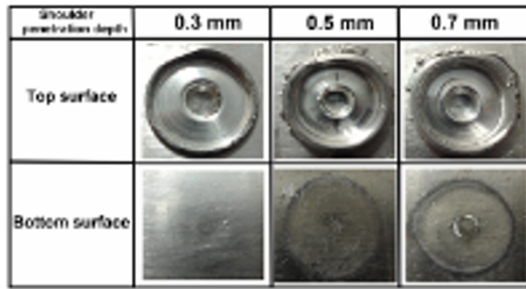


Fig. 7. The effect of shoulder penetration depth on surface appearance of welded specimens at 630 rpm rotational speed.

### 3.1 Surface appearance

The effects of the tool rotational speed and the shoulder penetration depth on the surface appearance is shown in Figs. 6 and 7, respectively. As seen, increasing rotational speed and shoulder penetration depth, has changed the surface appearance of the welds, especially at rotational speed of 1600 rpm. In addition, with increasing shoulder penetration depth and rotational speed, Z load (vertical force) not only increases [16] but also some extent of material are extruded from adjacent of shoulder, but as seen at 1600 rpm rotational speed, the effect of rotational speed on extruding materials more than penetration depth. It is well known that, there are circular traces with the diameters similar to those of the pin and the shoulder on the bottom surface of the lower sheet [11]. Based on the above mentioned results, with increasing rotational speed and the shoulder penetration depth, circular traces on the bottom surface of the lower sheet were increased. Furthermore, results indicates that rotational speed is a factor which has slight effect on the bottom surface while the shoulder penetration depth has a significant effect on the bottom surface of welded specimens.

### 3.2 Macrostructures

Fig. 8 depicts the effect of the rotational speed and shoulder penetration depth on macrostructure of the welded specimens. When a predetermined amount of tool was inserted into upper and lower sheets, stir zone formed in the vicinity of pin and the beneath of shoulder. With increasing rotational speed and

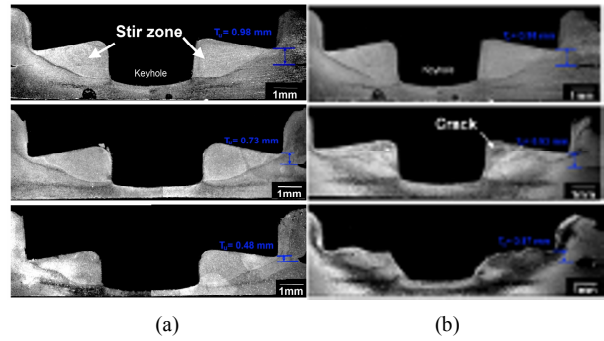


Fig. 8. Variation of stir zone as a function of (a) shoulder penetration depth; (b) rotational speed.

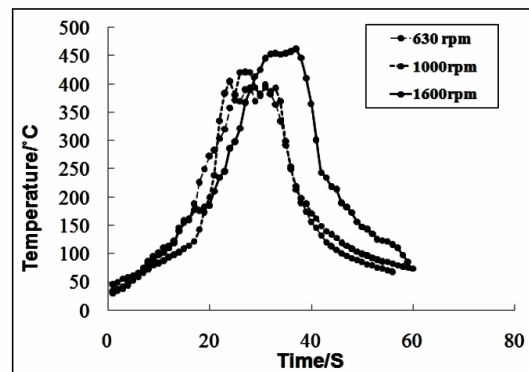


Fig. 9. Temperature profiles below the pin at different rotational speeds 630, 1000 and 1600 rpm.

the shoulder penetration depth, the frictional heat and the plastic flow of the base metals will be increase [18] which lead an increase in the stir zone area. As shown in the Fig. 8, with increasing the rotational speed and penetration depth, the stir zone area slightly increased. For example, stir zone area obtained in 630,1000 and 1600 rpm rotational speed in 0.3 mm penetration depth were 9.33,10.12,12.52 mm<sup>2</sup>, respectively while stir zone areas obtained in 0.3, 0.5 and 0.7 mm penetration depth at rotational speed 630 rpm were 9.33,10.98,11.82 mm<sup>2</sup>, respectively.

Also, it can be seen, when the penetration depth was 0.5 mm, the rotational speeds 1000 and 1600 rpm lead to the formation of micro cracks in the stir zone. The cracks were associated with local melting Al<sub>2</sub>CuMg phase that melted at temperature of 490°C. In Fig. 9, the temperature profile below the pin is shown at different rotational speeds of 630,1000 and 1600 rpm at constant shoulder penetration depth of 0.3 mm. As seen, with increasing tool rotational speed, the temperature rose up. For example with increasing rotational speed from 630 to 1600 rpm, temperature rose up from 399°C to 462°C, respectively. The existence of these temperature profiles are due to the frictional heat which is due to the increase in the tool rotational speed and shoulder penetration depth and this temperature profiles are also the main reason of increasing stir zone area.

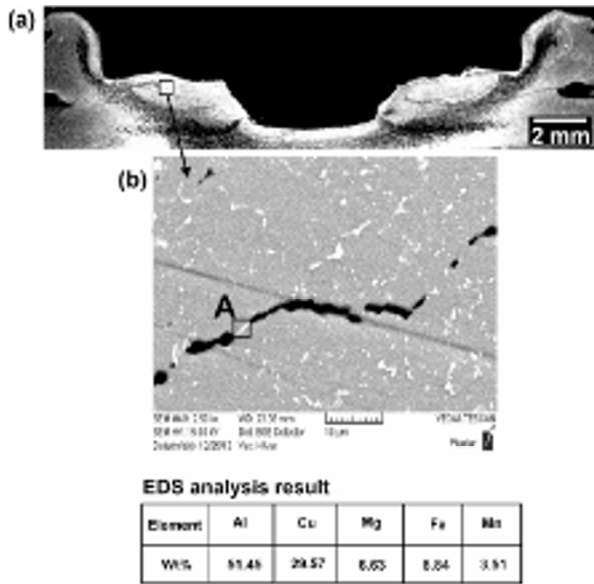


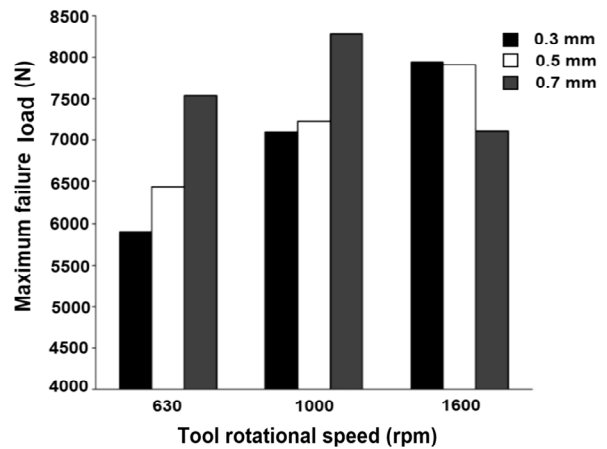
Fig. 10. (a) SEM micrograph from crack in the stir zone by using 1600 rpm; (b) magnification of location A, along EDS analysis result.

Figs. 10(a) and (b) depicts the macrostructure and SEM images of formed crack resulted to local melting at rotational speed of 1600 rpm and shoulder penetration depth of 0.3 mm, respectively. The joint microstructure depicts that the local melting of the Al<sub>2</sub>CuMg phase occurs in the stir zone [19]. The energy-dispersive spectroscopy (EDS) analyses indicated the presence of Cu, Mg, Fe and Mn in the crack walls. As it can be seen in the Fig. 8, increasing rotational speed and shoulder penetration depth caused a decrease in the thickness of the upper sheet under the shoulder indentation (Tu). These results depicts that increasing rotational speed and shoulder penetration depth led to an increase in the plastic flow of materials and consequently an increase in the stir zone area and formation of the cracks in the stir zone. Indeed, at rotational speed of 630 rpm, with increasing shoulder penetration depth, no defect was observed in the stir zone.

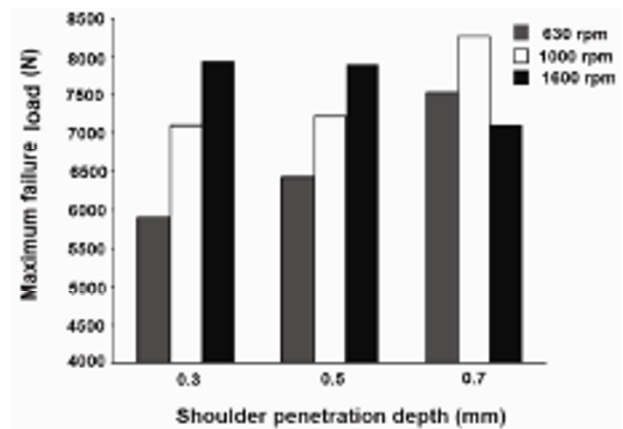
**3.3 Maximum failure load**

Figs. 11(a) and (b) compares the effect of the rotational speed and the shoulder penetration depth on the average maximum failure load, respectively. The stir zone area determines the strength of joints in the friction stir spot welding [15]. Maximum load of about 8282 N was obtained by using 1000 rpm rotational speed and 0.7 mm penetration depth.

As shown, with increasing rotational speed from 630 to 1600 rpm at 0.3 mm penetration depth, maximum failure load 25% increased. At rotational speed of 1600 rpm, the maximum failure load reached the maximum of 7535 N at 0.3 mm penetration depth. The reason of this behavior can be attributed to increasing stir zone area due to the fact that frictional heat and plastic flow of material are intensified by increasing



(a)



(b)

Fig. 11. The average maximum failure load as function of (a) tool rotational speed; (b) shoulder penetration depth.

rotational speed but while at 0.7 mm penetration depth, at first it increased and then 5% decreases.

Decreasing in maximum failure load is due to the excessive thinning of the upper sheet [18]. Also, as shown in Fig. 11(b), increasing shoulder penetration depth resulted in increasing the failure load because of the larger area of the stir zone.

As shown in Fig. 11(b), by increasing shoulder penetration depth for specimen welded at 630 and 1000 rpm rotational speed increased the failure load while at 1600 rpm rotational speed failure load reduces slightly. For example, at 1000 rpm rotational speed, increasing penetration depth from 0.3 to 0.7 mm leads to increase of 15% failure load.

These results indicated that there were a relationship between the stir zone area, the failure load and Tu. Indeed, the tool rotational speed is effective parameter and with increasing tool rotational speed, the different failure load between 0.3 and 0.5 mm penetration depth decreases. Furthermore, the results indicated that the effect of increasing shoulder penetration depth on the failure load is more remarkable than the rotational speed.

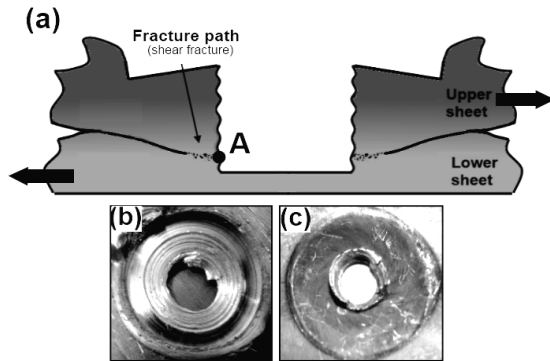


Fig. 12. (a) Schematic of the crack propagation path under tensile shear loading in shear fracture mode and also the top view of sheets after final fracture in (b) upper sheet; (c) lower sheet at 630 rpm rotational speed and 0.3 mm shoulder penetration depth. The arrows indicate the loading direction.

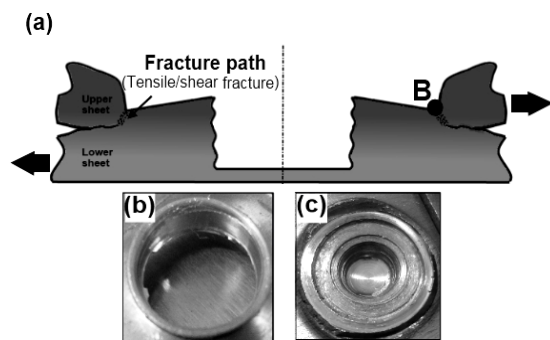


Fig. 13. (a) Schematic of the crack propagation path under tensile shear loading in tensile shear fracture mode and also the top view of sheets after final fracture in (b) upper sheet; (c) lower sheet at 1000 rpm rotational speed and 0.7 mm shoulder penetration depth. The arrows indicate the loading direction.

### 3.4 Failure modes

Figs. 12 and 13 depict the effects of the rotational speed and the shoulder penetration depth on failure modes in friction stir spot welding specimens under tensile shear loading. In this study, two types of failure modes were observed under tensile shear loading, including the shear failure mode and the tensile shear failure mode. In friction stir spot welding and under the tensile shear loading, the crack was propagated in the interface of upper and lower sheets [17]. In the shear failure mode (see Fig. 12), final fracture occurs in the location A, in the vicinity of the keyhole. Increasing the tool rotational speed only led to shear failure mode that in Figs. 12(a)-(c), respectively, schematic of crack propagation path and also the top view of sheets are depicted after final fracture in upper and lower sheets. In tensile shear failure mode (see Fig. 13), similar to shear failure mode, the crack initiated from the interface of upper and lower sheets and then propagates toward shoulder indentation and final fracture occurs in the location B. As seen in Figs. 13(a)-(c), respectively, the final fracture occurs at the shoulder indentation.

These results indicate that in case of the shoulder penetration

depth of 0.3 mm, shear failure mode occurs and the rotational speed does not play a major role in determining the type mode of the failure while by increasing shoulder penetration depth the failure mode changes from shear mode in the vicinity of the keyhole to tensile shear failure mode at shoulder indentation. According to the mentioned results, shoulder penetration depth was main reason of changing the failure mode.

### 4. Conclusions

The effect of shoulder penetration depth and tool rotational speed on the characteristics of friction stir spot welding of aluminum 2024-T3 is investigated. The important results obtained can be summarised as follows:

- (1) The surface appearance of welded joint depicts that the effect of shoulder penetration depth on the bottom surface is significantly more of the tool rotational speed.
- (2) The stir zone area is significantly affected by the tool rotational speed and the shoulder penetration depth.
- (3) Maximum failure load increases with increasing tool rotational speed and the shoulder penetration depth, but the effect of the shoulder penetration depth is significantly more of the tool rotational speed.
- (4) Two different failure modes are observed under tensile shear loadings, the shear fracture mode and the tensile shear fracture mode.

### Acknowledgements

This work was supported by Novin Sazan industrial group. The authors would like to thank Mr. Rasool Paidar, Mr. Ali Poshteban and Miss. Azam Abbasi for beneficial discussions and Miss Mahsa Laali Sarab for financial support.

### Nomenclature

- $T_u$  : The thickness of the upper sheet  
 SEM : Scanning electron microscopy  
 RPM : Round pair minute  
 FSSW : Friction stir spot welding  
 EDS : Energy dispersive X-ray spectroscopy  
 $T$  : Temperature

### References

- [1] R. Hancock, Friction welding of aluminum cuts energy cost by 99%, *Welding Journal*, 83 (2004) 40.
- [2] P. C. Lin, J. Pan and T. Pan, Failure modes and fatigue life estimations of spot friction welds in lap-shear specimens of aluminium 6111-T4 sheets. Part 2: Welds made by a flat tool, *Int. J. Fatigue*, 30 (2008) 90-105.
- [3] C. Herbelot, T. D. Hoang, A. Imad and N. Benseddiq, Damage mechanisms under tension shear loading in friction stir spot welding, *Sci. Technol. Weld. Join.*, 15 (2010) 688-693.
- [4] V. X. Tran, J. Pan and T. Pan, Effects of processing time on strengths and failure modes of dissimilar spot friction welds

- between aluminum 5754-O and 7075-T6 sheets, *J. Mater. Process. Technol.*, 209 (2009) 3724-3739.
- [5] S. Hirasawaa, H. Badarinarayan, K. Okamoto, T. Tomimura and T. Kawanami, Analysis of effect of tool geometry on plastic flow during friction stir spot welding using particle method, *J. Mater. Process. Technol.*, 210 (2010) 1455-1463.
- [6] S. Lathabai, M. J. Painter, G. M. D. Cantin and V. K. Tyagi, Friction spot joining of an extruded Al-Mg-Si alloy, *Scripta Mater.*, 55 (2006) 899-902.
- [7] Y. Tozaki, Y. Uematsu and K. Tokaji, Effect of tool geometry on microstructure and static strength in friction stir spot welded aluminium alloys, *Int. J. Mach. Tools. Manuf.*, 47 (2007) 2230-2236.
- [8] T. Pan, A. Joaquin, D. E. Wilkosz, L. Reatherford, J. M. Nicholson and Z. Fengm, Spot friction welding for sheet aluminum joining, *In: Proceedings of the 5th international symposium of friction stir welding*, Metz, France (2004).
- [9] M. Fujimoto, M. Inuzuka, M. Nishio and Y. Nakashima, Development of friction spot joining (Report 1)-cross sectional structures of friction spot joints, *The National Meeting of Japan Welding Society*, Japan (2004) 4-5.
- [10] M. Fujimoto, M. Inuzuka, M. Nishio and Y. Nakashima, Development of friction spot joining (Report 1)- mechanical properties of friction spot joints, *The National Meeting of Japan Welding Society*, Japan (2004) 6-7.
- [11] S. O. Yoon, M. S. Kang, Y. J. Kwon, S. T. Hong, D. H. Park, K. H. Lee, K. H. Lim and J. D. Seo, Influences of tool penetration speed and tool penetration depth on friction spot joining of AA5454-O aluminum alloy plates with different thicknesses. *Trans. Nonferrous. Met. Soc. China*, 22 (2012) 629-633.
- [12] N. Pathak, K. Bandyopadhyay, M. sarangi and S. K. Panda, Microstructure and mechanical performance of friction stir spot- welded aluminum-5754 sheets, *J. Mater. Eng. Perform.*, 22 (2012) 131-144.
- [13] D. Mitlin, V. Radmilovic, T. Pan, J. Chen, Z. Feng and M. L. Santalla, Structure properties relations in spot friction welded 6111 aluminium, *Mater. Sci. Eng. A*, 441 (2006) 79-96.
- [14] Z. Zhang, X. Yang, J. Zhang, G. Zhou, X. Xu and R. Zou, Effect of welding parameters on microstructure and mechanical properties of friction stir spot welded 5052 aluminum alloy, *Mater. Des.*, 32 (2011) 4462-4470.
- [15] A. Gerlich, T. H. North and M. Yamamoto, Local melting and cracking in Al 7075-T6 and Al 2024-T3 friction stir spot welds, *Sci. Technol. Weld. Join.*, 12 (2007) 472-480.
- [16] H. Badarinarayan, Y. Shi, X. Li and K. Okamoto, Effect of tool geometry on hook formation and static strength of friction stir spot welded aluminum 5754-O sheets, *Int. J. Mach. Tools. Manuf.*, 49 (2009) 814-823.
- [17] D. A. Wang, C. W. Chao, P. C. Lin and J. Y. Uan, Mechanical characterization of friction stir spot microwelds, *J. Mater. Process. Technol.*, 14 (2010) 1942-1948.
- [18] M. K. Bilici and A. I. Yukler, Effects of welding parameters on friction stir spot welding of high density polyethylene sheets, *Mater. Des.*, 33 (2012) 545-550.
- [19] A. Gerlich, P. Su, M. Yamamoto and T. H. North, Effect of

welding parameters on the strain rate and microstructure of friction stir spot welded 2024 aluminium alloy, *J. Mat. Sci.*, 42 (2007) 5589-5601.



**Moslem Paidar** received his B.S. in Materials Engineering from Shahrekord University, Iran, in 2010. Then, He received his M.S. degrees from Graduate School of Materials Engineering, Tehran Science and Research Branch, Islamic Azad University, Tehran, Iran in 2013. Mr. Paidar is currently Ph.D student in South Tehran Branch, Islamic Azad University in Tehran, Iran. Mr. Paidar's research interests include Laser Beam Welding, Diffusion Welding, Welding-Brazing, Surface engineering, Brazing And Activated TIG for dissimilar materials and Light metals.



**Alireza Khodabandeh** is an assistant professor of Materials Engineering Department at Science and Research Branch of Islamic Azad University in Tehran, Iran, where he has been a faculty member since 2008. He received his B.S. degree in Materials Engineering from Shiraz University, Iran, at 1994. He also received his M.Sc. in Materials Engineering from Tarbiat Modares University, Iran, at 1997 and then he completed his Ph.D. at 2005, from Tarbiat Modares University. His research interests lie in the area of Physical Properties of Materials with a focus on Solid State Transformation, Diffusion in Solids and Microstructure.



**Hamidreza Najafi** received his B.S. degree in Materials Engineering from University of Tehran, Iran, in 1999. Then, He received his M.S. degree from Sharif University of Technology, Iran, 2001. He graduated in 2007 with a Ph.D. in Materials Engineering from University of Tehran, Iran. Dr. Najafi is currently an Assistant Professor at Department of Materials Engineering at Tehran Science and Research Branch, Islamic Azad University, Tehran, Iran. His research interests include phase transformations and materials characterization.



**Alireza Sabour rouh-Aghdam** an associate professor of Materials Engineering Department at Tarbiat Modares University in Iran, Tehran. He received his M.S. degree from Germany, 1988. He graduated in 1993 with a Ph.D. in Materials Engineering from in German. Dr. Sabour rouh-Aghdam is faculty member of Department at Tarbiat Modares University since 1995. His research interests include Surface engineering and materials characterization.